

Tensor-to-Scalar Transition in the Nucleon-Nucleon Interaction Mapped by $^{12}\text{C}(e,e'pn)$ Measurements

I. Korover,¹ J. R. Pybus,² A. Schmidt,^{3,2} F. Hauenstein,^{2,4} M. Duer,⁵ O. Hen,^{2,*} E. Piassetzky,⁵ L.B. Weinstein,⁴ D.W. Higinbotham,⁶ S. Adhikari,⁷ K. Adhikari,⁸ M.J. Amarian,⁴ Giovanni Angelini,⁹ H. Atac,¹⁰ L. Barion,¹¹ M. Battaglieri,^{6,12} A. Beck,^{2,†} I. Bedlinskiy,¹³ Fatiha Benmokhtar,¹⁴ A. Bianconi,^{15,16} A.S. Biselli,^{17,18} S. Boiarinov,⁶ W.J. Briscoe,⁹ W.K. Brooks,^{19,6} D. Bulumulla,⁴ V.D. Burkert,⁶ D.S. Carman,⁶ A. Celentano,¹² P. Chatagnon,²⁰ T. Chetry,⁸ L. Clark,²¹ B. Clary,²² P.L. Cole,^{23,24,25} M. Contalbrigo,¹¹ V. Crede,²⁶ R. Cruz-Torres,² A. D'Angelo,^{27,28} R. De Vita,¹² M. Defurne,²⁹ A. Denniston,² A. Deur,⁶ S. Diehl,²² C. Djalali,^{30,31} R. Dupre,²⁰ H. Egiyan,⁶ M. Ehrhart,³² A. El Alaoui,¹⁹ L. El Fassi,⁸ L. Elouadrhiri,⁶ P. Eugenio,²⁶ R. Fersch,^{33,34} A. Filippi,³⁵ T. Forest,²⁴ G. Gavalian,^{6,36} F.X. Girod,⁶ E. Golovatch,³⁷ R.W. Gothe,³¹ K.A. Griffioen,³⁴ M. Guidal,²⁰ K. Hafidi,³² H. Hakobyan,^{19,38} N. Harrison,⁶ M. Hattawy,⁴ F. Hauenstein,⁴ T.B. Hayward,³⁴ D. Heddle,^{33,6} K. Hicks,³⁰ M. Holtrop,³⁶ Y. Ilieva,^{31,9} D.G. Ireland,²¹ E.L. Isupov,³⁷ D. Jenkins,³⁹ H.S. Jo,⁴⁰ K. Joo,²² S. Joosten,³² D. Keller,⁴¹ M. Khachatryan,⁴ A. Khanal,⁷ M. Khandaker,^{42,‡} A. Kim,²² C.W. Kim,⁹ F.J. Klein,²⁵ V. Kubarovsky,^{6,43} L. Lanza,²⁷ M. Leali,^{15,16} P. Lenisa,^{11,44} K. Livingston,²¹ V. Lucherini,⁴⁵ I. J. D. MacGregor,²¹ D. Marchand,²⁰ N. Markov,⁶ L. Marsicano,¹² V. Mascagna,^{46,16,§} B. McKinnon,²¹ S. Mey-Tal Beck,^{2,†} T. Mineeva,¹⁹ M. Mirazita,⁴⁵ A. Movsisyan,¹¹ C. Munoz Camacho,²⁰ B. Mustapha,³² P. Nadel-Turonski,⁶ K. Neupane,³¹ G. Niculescu,⁴⁷ M. Osipenko,¹² A.I. Ostrovidov,²⁶ M. Paolone,¹⁰ L.L. Pappalardo,^{11,44} R. Paremuzyan,³⁶ E. Pasyuk,⁶ W. Phelps,³³ O. Pogorelko,¹³ J.W. Price,⁴⁸ Y. Prok,^{4,41} D. Protopopescu,²¹ B.A. Raue,^{7,6} M. Ripani,¹² J. Ritman,⁴⁹ A. Rizzo,^{27,28} G. Rosner,²¹ J. Rowley,³⁰ F. Sabatié,²⁹ C. Salgado,⁴² R.A. Schumacher,¹⁸ E.P. Segarra,² Y.G. Sharabian,⁶ U. Shrestha,³⁰ D. Sokhan,²¹ O. Soto,⁴⁵ N. Sparveris,¹⁰ S. Stepanyan,⁶ I.I. Strakovsky,⁹ S. Strauch,^{31,9} J.A. Tan,⁴⁰ N. Tyler,³¹ M. Ungaro,^{6,43} L. Venturelli,^{15,16} H. Voskanyan,³⁸ E. Voutier,²⁰ T. Wang,⁵⁰ D. Watts,⁵¹ X. Wei,⁶ M.H. Wood,^{52,31} N. Zachariou,⁵¹ J. Zhang,⁴¹ Z.W. Zhao,⁵³ and X. Zheng⁴¹

(The CLAS Collaboration)

¹Nuclear Research Center Negev, Be'er Sheva 84190, Israel

²Massachusetts Institute of Technology, Cambridge, MA 02139, USA

³The George Washington University, Washington, DC, 20052, USA

⁴Old Dominion University, Norfolk, VA 23529, USA

⁵School of Physics and Astronomy, Tel Aviv University, Tel Aviv 69978, Israel

⁶Thomas Jefferson National Accelerator Facility, Newport News, VA 23606, USA

⁷Florida International University, Miami, Florida 33199

⁸Mississippi State University, Mississippi State, MS 39762-5167

⁹The George Washington University, Washington, DC 20052

¹⁰Temple University, Philadelphia, PA 19122

¹¹INFN, Sezione di Ferrara, 44100 Ferrara, Italy

¹²INFN, Sezione di Genova, 16146 Genova, Italy

¹³National Research Centre Kurchatov Institute - ITEP, Moscow, 117259, Russia

¹⁴Duquesne University, 600 Forbes Avenue, Pittsburgh, PA 15282

¹⁵Università degli Studi di Brescia, 25123 Brescia, Italy

¹⁶INFN, Sezione di Pavia, 27100 Pavia, Italy

¹⁷Fairfield University, Fairfield CT 06824

¹⁸Carnegie Mellon University, Pittsburgh, Pennsylvania 15213

¹⁹Universidad Técnica Federico Santa María, Casilla 110-V Valparaíso, Chile

²⁰Université Paris-Saclay, CNRS/IN2P3, IJCLab, 91405 Orsay, France

²¹University of Glasgow, Glasgow G12 8QQ, United Kingdom

²²University of Connecticut, Storrs, Connecticut 06269

²³Lamar University, 4400 MLK Blvd, PO Box 10009, Beaumont, Texas 77710

²⁴Idaho State University, Pocatello, Idaho 83209

²⁵Catholic University of America, Washington, D.C. 20064

²⁶Florida State University, Tallahassee, Florida 32306

²⁷INFN, Sezione di Roma Tor Vergata, 00133 Rome, Italy

²⁸Università di Roma Tor Vergata, 00133 Rome Italy

²⁹IRFU, CEA, Université Paris-Saclay, F-91191 Gif-sur-Yvette, France

³⁰Ohio University, Athens, Ohio 45701

³¹University of South Carolina, Columbia, South Carolina 29208

³²Argonne National Laboratory, Argonne, Illinois 60439

³³Christopher Newport University, Newport News, Virginia 23606

³⁴College of William and Mary, Williamsburg, Virginia 23187-8795

³⁵INFN, Sezione di Torino, 10125 Torino, Italy

³⁶University of New Hampshire, Durham, New Hampshire 03824-3568

³⁷Skobeltsyn Institute of Nuclear Physics, Lomonosov Moscow State University, 119234 Moscow, Russia

³⁸Yerevan Physics Institute, 375036 Yerevan, Armenia

³⁹Virginia Tech, Blacksburg, Virginia 24061-0435

⁴⁰Kyungpook National University, Daegu 41566, Republic of Korea

⁴¹University of Virginia, Charlottesville, Virginia 22901

⁴²Norfolk State University, Norfolk, Virginia 23504

⁴³Rensselaer Polytechnic Institute, Troy, New York 12180-3590

⁴⁴Università di Ferrara, 44121 Ferrara, Italy

⁴⁵INFN, Laboratori Nazionali di Frascati, 00044 Frascati, Italy

⁴⁶Università degli Studi dell'Insubria, 22100 Como, Italy

⁴⁷James Madison University, Harrisonburg, Virginia 22807

⁴⁸California State University, Dominguez Hills, Carson, CA 90747

⁴⁹Institute für Kernphysik (Juelich), Juelich, Germany

⁵⁰Beihang School of Physics, Beihang University, Beijing 100191, China

⁵¹University of York, York YO10 5DD, United Kingdom

⁵²Canisius College, Buffalo, NY

⁵³Duke University, Durham, North Carolina 27708-0305

(Dated: April 25, 2022)

The strong nuclear interaction is probed at short-distance and high-momenta using new measurements of the $^{12}\text{C}(e, e'p)$ and $^{12}\text{C}(e, e'pn)$ reactions, at high- Q^2 and $x_B > 1$. The data span a missing-momentum range of 300–850 MeV/c and is predominantly sensitive to the dominant proton-neutron short-range correlated (SRC) pairs and complements previous $^{12}\text{C}(e, e'pp)$ measurements. The data are well reproduced by theoretical calculations using the Generalized Contact Formalism with both chiral and phenomenological nucleon-nucleon (NN) interaction models. This agreement, observed here for the first time, suggests that the measured high missing-momentum protons up to 850 MeV/c belonged to SRC pairs. The measured $^{12}\text{C}(e, e'pn) / ^{12}\text{C}(e, e'p)$ ratio is consistent with a decrease in the fraction of proton-neutron SRC pairs with increasing missing-momentum. This confirms the transition from an isospin-dependent tensor NN interaction at ~ 400 MeV/c to an isospin-independent scalar interaction at high-momentum around ~ 800 MeV/c.

High momentum-transfer electron- and proton-scattering measurements [1–10], as well as many-body *ab initio* calculations [11–18], have shown that nucleons in the nuclear ground state form temporary pairs with large relative momentum and smaller center-of-mass (CM) momentum. These are called Short-Range Correlated (SRC) pairs [19, 20]. The existence and characteristics of SRC pairs are related to outstanding issues in particle, nuclear, and astrophysics, including the modification of the internal structure of nucleons bound in atomic nuclei (i.e., the EMC effect) [20–26], matrix elements used to interpret searches for neutrinoless double beta decay [27–33], scale separation and factorization of many-body nuclear wavefunctions [34–42], nuclear charge radii [43], and the nuclear symmetry energy governing neutron star properties [44–47].

A well-established feature of SRC pairs is the predominance of pn -SRC pairs in the missing momentum range of 300–600 MeV/c [1–8]. The cause is understood to be the preference of spin-1 pn -pairs by the tensor part of the NN interaction, which is much stronger than the scalar part of the interaction at these missing momenta [11, 12, 48]. At higher missing momentum the scalar repulsive core of the NN interaction should become much more important and increase the fraction of proton-proton (pp) SRC

pairs [5, 10, 19, 20]. Quantifying this tensor-to-scalar transition provides valuable insight into the nature of the strong nuclear interaction at short-distances, which determines the properties of dense astrophysical systems such as neutron stars.

Such a transition was recently reported in measurements of the $^{12}\text{C}(e, e'p)$ and $^{12}\text{C}(e, e'pp)$ reactions, where the fraction of two-proton knockout events was observed to increase as a function of missing momentum [10]. However, this interpretation in terms of the underlying NN interaction assumed (1) that all high missing-momentum protons belonged to $2N$ -SRC pairs, and (2) reaction effects were properly accounted for, primarily (n, p) single-charge exchange (SCX) processes. Even modest SCX can significantly distort the $(e, e'pp)$ reaction due to the predominance of pn -SRC pairs, because the observed $(e, e'pp)$ events can originate from pn -SRC pairs in which the neutron undergoes SCX. Therefore, while experimentally simpler, SRC measurements via the $(e, e'pp)$ reaction are subject to sizable model-dependent corrections and are based on an assumption of SRC dominance that has not yet been proven for momenta above 600 MeV/c.

Here we present the results of a direct measurement of pn -SRC pairs using the $^{12}\text{C}(e, e'pn)$ and $^{12}\text{C}(e, e'p)$ reactions, which are minimally sensitive to SCX corrections

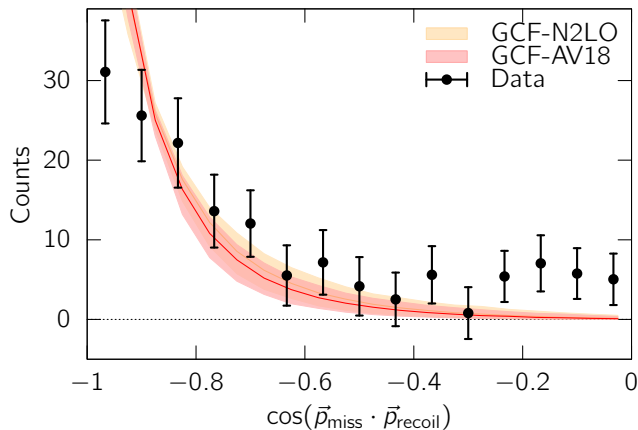


FIG. 1: Background-subtracted angular correlation between \vec{p}_{miss} and \vec{p}_{recoil} for data events passing $^{12}\text{C}(e, e'pn)$ cuts (points), compared with GCF predictions based on the AV18 and N2LO NN interactions (bands).

due to the small fraction of initial-state pp -SRC pairs. Combined with existing $^{12}\text{C}(e, e'pp)$ data [10] and theoretical calculations using the Generalized Contact Formalism (GCF) [37, 38, 42, 49], we establish the $2N$ -SRC dominance of the measured reactions and the observation of a scalar repulsive interaction at short distances.

The analysis is based on data collected in 2004 in Hall B of the Thomas Jefferson National Accelerator Facility (Jefferson Lab) in Virginia, USA, and were re-analyzed as part of the Jefferson Lab data-mining initiative [50]. A 5.01 GeV electron beam was directed on deuterium, carbon, aluminum, iron, and lead targets [51]. Due to statistical limitations, only carbon data are presented here. The CEBAF Large Acceptance Spectrometer (CLAS) [52] was used to detect the scattered electrons, knocked-out protons, and recoil neutrons.

CLAS utilized a toroidal magnetic field and six independent sets of drift chambers (DCs) [53], time-of-flight (TOF) scintillation counters [54], Cherenkov counters (CCs) [55], and electromagnetic calorimeters (EC) [56] for charged particle detection and identification. Charged particle momenta were inferred from their reconstructed trajectories within the magnetic field. Electrons were identified by requiring a signal in the CC, as well as a characteristic energy deposition in the EC. Protons were identified through correlations between momentum and flight time. The TOF and DC polar angular acceptance was $8^\circ \leq \theta \leq 140^\circ$ and the azimuthal angular acceptance ranged from 50% at small polar angles to 80% at larger polar angles. The EC and CC polar angular acceptance was limited to $< 45^\circ$.

Neutrons with momenta of 200–1000 MeV/c were detected in the TOF counters by requiring a hit with energy deposition above threshold (nominally 8 MeVee), no matching charged-particle track in the drift chambers

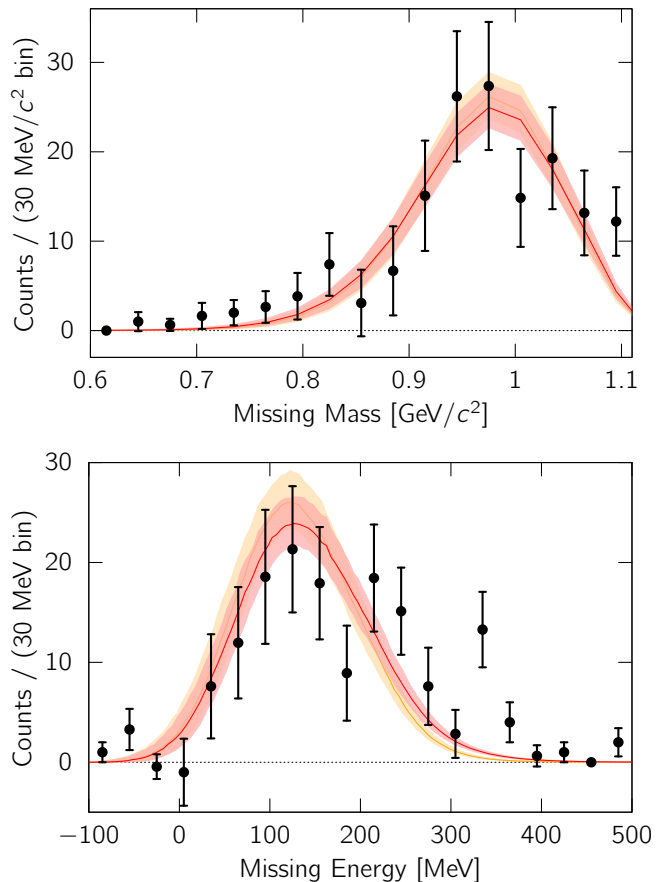


FIG. 2: Background-subtracted missing mass (top) and missing energy (bottom) distribution for data events passing the $^{12}\text{C}(e, e'pn)$ selection cuts (points), compared with GCF predictions based on the AV18 and N2LO NN interactions (bands).

and a TOF that corresponds to $\beta < 0.75$. We only considered hits reconstructed inside a fiducial region that excluded 10 cm from the ends of all scintillator paddles. Our results are not sensitive to the exact use of 10 cm. Neutron momenta were determined by time-of-flight, with a typical resolution of 25–40 MeV/c.

The neutron detection efficiency was determined using the over-constrained $d(e, e'p)n$ and $d(e, e'pn)$ reactions. The efficiency was extracted for different TOF energy deposition thresholds in the range of 4–10 MeVee and as a function of the recoil neutron momentum determined by the $d(e, e'p)n$ reaction. For momenta above 400 MeV/c, the typical efficiency was 4–5%. Between 200 and 400 MeV/c, the efficiency was somewhat lower, approximately 2–3%. We verified that the charged particle veto efficiency, using the DC tracking system, results in a negligible fraction of identified neutrons that are in fact charged particles that were not reconstructed in the DC tracking system. See online supplementary materials for additional details on the neutron identification, detection

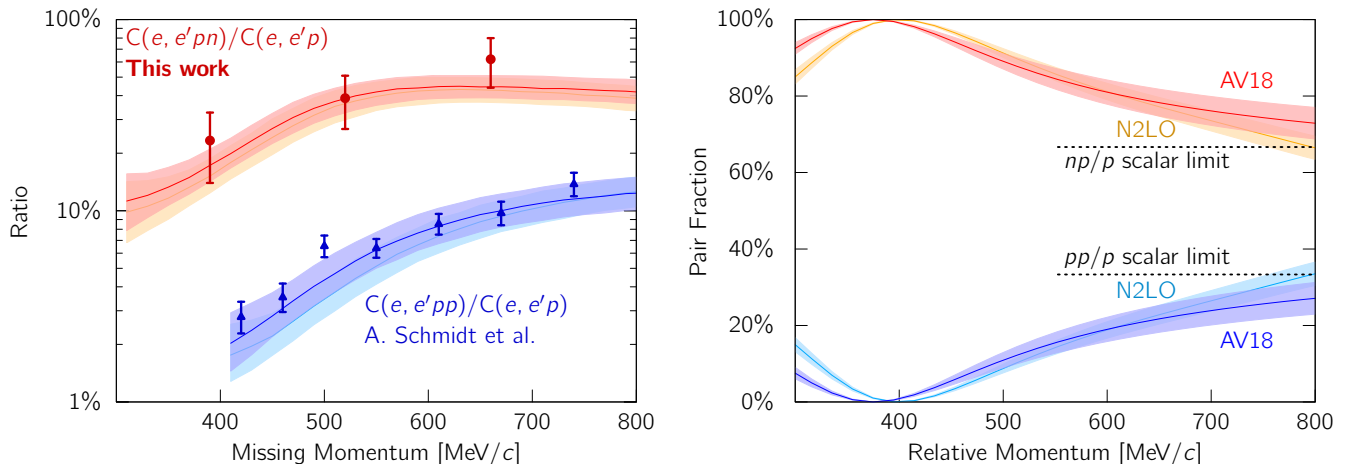


FIG. 3: Left: The measured fractions of triple coincidence events ($C(e, e'pN)/C(e, e'p)$), compared with GCF predictions accounting for the variety of effects that influence the measurement (e.g. CLAS detector acceptance, efficiency, and resolution, FSIs including SCX, and the event-selection procedure). The $C(e, e'pp)/C(e, e'p)$ data (blue triangles) are taken from Ref. [10], while the $C(e, e'pn)/C(e, e'p)$ data (red circles) are from this work. Right: The GCF prediction for the ground-state fractions of pn and pp pairs as a function of pair relative momentum, calculated using the AV18 and N2LO NN interactions. The dashed line marks the scalar limit, see text for details. The width of the GCF calculation bands shows their 68% confidence interval due to uncertainties on the model parameters.

efficiency, and momentum reconstruction resolution.

Similar to previous SRC studies [6–10], we considered events with scattered electron kinematics of $Q^2 \equiv |\vec{q}|^2 - \omega^2 > 1.5 \text{ GeV}^2/c^2$ and $x_B \equiv Q^2/2m_N\omega > 1.1$, where m_N is the nucleon mass, while \vec{q} and ω are the 3-momentum and energy transferred to the nucleus by the electron, respectively. Assuming the electron scatters from a single nucleon that does not reinteract as it leaves the nucleus with momentum \vec{p}_f , the initial nucleon momentum \vec{p}_i can be approximated as equal to the measured missing-momentum: $\vec{p}_i \approx \vec{p}_{\text{miss}} \equiv \vec{p}_f - \vec{q}$.

If the struck nucleon is part of a $2N$ -SRC pair, we interpret the reaction through the SRC break-up model where a correlated partner nucleon is assumed to exist as an on-shell spectator carrying momentum \vec{p}_{recoil} . For an SRC pair with center-of-mass momentum $\vec{p}_{CM} \equiv \vec{p}_i + \vec{p}_{\text{recoil}}$, the residual $A - 2$ system will carry momentum $-\vec{p}_{CM}$, and may carry excitation energy denoted here by E^* . We also define the missing energy, $E_{\text{miss}} \equiv m_N - m_A + \sqrt{(\omega + m_A - E_f)^2 - p_{\text{miss}}^2}$, where m_A is the mass of the target nucleus and E_f is the energy of the leading proton detected in the final state.

Following previous works [6–10], we selected $^{12}\text{C}(e, e'p)$ events in kinematics where the dominant reaction is the scattering off SRC pairs. Specifically, $^{12}\text{C}(e, e'p)$ events were required to have $x_B > 1.1$ which suppresses contributions from isobar currents, $300 < p_{\text{miss}} < 1000 \text{ MeV}/c$ that enhances contributions from interactions with high initial momentum nucleons, an angle between \vec{p}_f and \vec{q} smaller than 25° , $0.62 < |\vec{p}_f|/|\vec{q}| < 0.96$ that allows identifying a leading nucleon, and $M_{\text{miss}} \equiv$

$\sqrt{(q^\mu - p_f^\mu + 2m_N)^2} < 1.1 \text{ GeV}/c^2$ that suppress resonance productions.

Triple coincidence $^{12}\text{C}(e, e'pn)$ events were selected from the $^{12}\text{C}(e, e'p)$ event sample by requiring a neutron candidate in the TOF counters. We only considered neutrons with momentum between 300 and 1000 MeV/c. The triple coincidence signal sits on top of a similar-size uncorrelated random background. This background is uniformly random in neutron hit time, allowing it to be estimated from off-time neutrons and subtracted. More details on the event selection and background subtraction can be found in the online supplementary materials.

Figure 1 shows the cosine of the angle between \vec{p}_{miss} and \vec{p}_{recoil} for $^{12}\text{C}(e, e'pn)$ events after random coincidence background subtraction. While the recoil neutron selection criteria do not place any angular requirements, the measured distribution shows the back-to-back correlation characteristic of SRC breakup events.

The measured distributions are compared to theoretical predictions based on the GCF [37, 38, 42, 49] using the local AV18 [57] and N2LO(1.0) [58] NN interaction models. The GCF assumes scale-separation between the short-distance interactions within an SRC pair, and the long-range interactions between the pair and the rest of the nucleus, as well as their mutual separation from the ultra-short distance scale associated with the high-energy virtual photon probe. This scale separation permits a factorized approximation for describing the scattering cross-section, in which the hard break-up of an SRC pair proceeds via a reaction in which the virtual photon is absorbed by a single nucleon in an SRC pair,

knocking it out of the nucleus and leaving its correlated partner nucleon to recoil from the nucleus.

Several ingredients are necessary to construct the GCF cross-section [49]. We used the off-shell electron-nucleon cross-section from Ref. [59]. GCF parameters describing SRC pairs in the nuclear ground state are the same as in Ref. [10] and include the fraction of SRC pairs in different spin-isospin channels (known as *nuclear contacts*) [37, 38, 42], the characteristic width of the SRC pair CM momentum distribution [9], and the possible excitation range of the residual $A - 2$ nuclear system E^* . Additionally, we accounted for Final State Interactions (FSIs) including Single Charge Exchange (SCX) and nuclear transparency using the Glauber approximation from Ref. [60], which was previously shown to well-reproduce experimental data [61–63].

To compare the GCF calculations with our data, we used Monte Carlo integration to convolute the calculated cross-sections through a model of the CLAS detector, which included acceptance, efficiency and resolution effects. We applied the same event selection criteria as the ones applied to the data. This allows a direct comparison of the theory to the data, leaving all model-dependent assumptions on the calculation alone. See ref. [49] for details.

Systematic uncertainties associated with the GCF predictions were estimated by repeating the theoretical calculations with randomly sampled model parameters from a distribution centered around the parameter’s nominal value with a width defined by its uncertainty. We also varied the momentum resolutions for electrons, protons, and neutrons in CLAS based on their uncertainties and used two prescriptions for the off-shell electron-nucleon cross-section known as cc1 and cc2 from Ref. [59].

Figure 2 shows the background-subtracted distributions of M_{miss} and E_{miss} for $^{12}\text{C}(e, e'pn)$ events, compared with the GCF calculations. The width of the GCF band represents a 68% confidence interval associated with the uncertainties due to the model parameters. Both measured distributions are well-reproduced by the calculation.

The resulting $^{12}\text{C}(e, e'pn) / ^{12}\text{C}(e, e'p)$ yield ratio as a function of p_{miss} is shown in Fig. 3 (left panel), compared with GCF calculations. The data error bars show the quadratic sum of the statistical uncertainty and the systematic uncertainty. The latter is dominated by uncertainties in the determination of the absolute neutron detection efficiency (see online supplementary materials for details). The GCF calculations agree well with the data over the missing momentum range probed by this study using either NN potential. This agreement of the cross-section ratios supports the validity of the GCF description of the ground state.

The underlying ground-state fraction of pn -SRC pairs relative to all pp - and pn -SRC pairs from the same GCF calculation is shown in Fig. 3 (right panel) as a function of

pair relative momentum. The pn -SRC fraction is 100% at $p_{\text{miss}} \approx 400$ MeV/c and decreases to about 70% at $p_{\text{miss}} \approx 800$ MeV/c, showing the transition from tensor to scalar dominance.

The complete np -SRC dominance at 400 MeV/c is caused by a dip in the pp wave function, which is absent for spin-1 pn pairs due to the tensor interaction [11, 12, 48]. The 70% fraction at large relative momenta is consistent with simple pair counting due to a purely scalar NN interaction. In a symmetric nucleus such as ^{12}C , scalar interactions lead to equal abundance of pairs in all spin-isospin combinations. This implies that the number of spin-1 pn -SRC pairs should be three times the number of spin-0 pn -pairs, (and, by symmetry, spin-0 pp - and nn -pairs), due to the three possible projections of the spin-1 state. Simple counting would suggest a ratio of pn to $pn + pp$ pairs of $(N_{pn}^{s=0} + N_{pn}^{s=1}) / (2N_{pp}^{s=0} + N_{pn}^{s=0} + N_{pn}^{s=1}) = (1 + 3) / (2 + 1 + 3) = 2/3$.

For completeness, Fig. 3 (left panel) also shows the results of the recent study of pp -SRC by Ref. [10] (blue triangles). The data are compared with the same GCF calculations that well-reproduce both pn and pp channels. The large predominance of pn -SRC pairs shown in Fig. 3 (right panel) makes it clear that even a small probability of SCX reactions would lead to a sizable population of the measured $^{12}\text{C}(e, e'pp)$ events originating from breakup of pn -SRC pairs. Therefore, the consistency of both $^{12}\text{C}(e, e'pn)$ and $^{12}\text{C}(e, e'pp)$ data with the GCF calculations (1) confirms that all measured high missing-momentum protons belong to either pp - or pn -SRC pairs and (2) supports SCX corrections applied in the $^{12}\text{C}(e, e'pp)$ analysis of Ref. [10].

To conclude, we report on new measurements of the $^{12}\text{C}(e, e'pn)$ reaction at very high missing-momentum. The data are compared with both recent $^{12}\text{C}(e, e'pp)$ measurements and GCF calculations. The agreement of the same GCF calculation with both $^{12}\text{C}(e, e'pn)$ and $^{12}\text{C}(e, e'pp)$ data indicates that within the uncertainty of the data, the measured reactions are dominated by interactions with $2N$ -SRC pairs and that reaction effects such as SCX, which has a large impact on the $^{12}\text{C}(e, e'pp)$ channel but a small impact on the $^{12}\text{C}(e, e'pn)$ channel, are accurately modeled.

The combination of all data and calculations confirms the observation of a transition of the NN interaction from a tensor-dominated region around relative momenta of 400 MeV/c to a predominantly scalar interaction around 800 MeV/c, validating the use of the NN interactions examined here in modeling of dense astrophysical systems such as neutron stars. Future extensions of the GCF to three-nucleon correlations as well as forthcoming measurements [64] of three-nucleon knockout reactions $A(e, e'pNN)$ will allow similar studies of the short-distance three-body interactions that are needed for a complete description of neutron stars [65].

We acknowledge the efforts of the staff of the Accel-

erator and Physics Divisions at Jefferson Lab that made this experiment possible. The analysis presented here was carried out as part of the Jefferson Lab Hall B Data-Mining project supported by the U.S. Department of Energy (DOE). The research was also supported also by the National Science Foundation, the Pazy Foundation, the Israel Science Foundation and the United Kingdom's Science and Technology Facilities Council (STFC). The Jefferson Science Associates operates the Thomas Jefferson National Accelerator Facility for the DOE, Office of Science, Office of Nuclear Physics under Contract No. DE-AC05-06OR23177.

* Contact Author hen@mit.edu

† On sabbatical leave from Nuclear Research Center Negev, Be'er Sheva 84190, Israel

‡ Current address: Idaho State University, Pocatello, Idaho 83209

§ Current address: Università degli Studi di Brescia, 25123 Brescia, Italy

- [1] A. Tang et al., *Phys. Rev. Lett.* **90**, 042301 (2003).
- [2] E. Piasetzky, M. Sargsian, L. Frankfurt, M. Strikman, and J. W. Watson, *Phys. Rev. Lett.* **97**, 162504 (2006).
- [3] R. Subedi et al., *Science* **320**, 1476 (2008).
- [4] R. Shneor et al., *Phys. Rev. Lett.* **99**, 072501 (2007).
- [5] I. Korover, N. Muangma, O. Hen, et al., *Phys. Rev. Lett.* **113**, 022501 (2014).
- [6] O. Hen et al. (CLAS Collaboration), *Science* **346**, 614 (2014).
- [7] M. Duer et al. (CLAS Collaboration), *Phys. Rev. Lett.* **122**, 172502 (2019), 1810.05343.
- [8] M. Duer et al. (CLAS Collaboration), *Nature* **560**, 617 (2018).
- [9] E. O. Cohen et al. (CLAS Collaboration), *Phys. Rev. Lett.* **121**, 092501 (2018), 1805.01981.
- [10] A. Schmidt et al. (CLAS Collaboration), *Nature* **578**, 540544 (2020).
- [11] R. Schiavilla, R. B. Wiringa, S. C. Pieper, and J. Carlson, *Phys. Rev. Lett.* **98**, 132501 (2007).
- [12] M. Alvioli, C. C. degli Atti, and H. Morita, *Phys. Rev. Lett.* **100**, 162503 (2008).
- [13] H. Feldmeier, W. Horiuchi, T. Neff, and Y. Suzuki, *Phys. Rev. C* **84**, 054003 (2011), 1107.4956.
- [14] M. Alvioli, C. Ciofi degli Atti, L. P. Kaptari, C. B. Mezzetti, and H. Morita, *Phys. Rev. C* **87**, 034603 (2013), 1211.0134.
- [15] R. B. Wiringa, R. Schiavilla, S. C. Pieper, and J. Carlson, *Phys. Rev. C* **89**, 024305 (2014).
- [16] J. Carlson, S. Gandolfi, F. Pederiva, S. C. Pieper, R. Schiavilla, K. E. Schmidt, and R. B. Wiringa, *Rev. Mod. Phys.* **87**, 1067 (2015).
- [17] T. Neff, H. Feldmeier, and W. Horiuchi, *Phys. Rev. C* **92**, 024003 (2015).
- [18] D. Lonardonì, A. Lovato, S. C. Pieper, and R. B. Wiringa, *Phys. Rev. C* **96**, 024326 (2017), 1705.04337.
- [19] C. Ciofi degli Atti, *Phys. Rept.* **590**, 1 (2015).
- [20] O. Hen, G. A. Miller, E. Piasetzky, and L. B. Weinstein, *Rev. Mod. Phys.* **89**, 045002 (2017).
- [21] L. B. Weinstein, E. Piasetzky, D. W. Higinbotham, J. Gomez, O. Hen, and R. Shneor, *Phys. Rev. Lett.* **106**, 052301 (2011).
- [22] O. Hen, E. Piasetzky, and L. B. Weinstein, *Phys. Rev. C* **85**, 047301 (2012).
- [23] O. Hen, D. W. Higinbotham, G. A. Miller, E. Piasetzky, and L. B. Weinstein, *Int. J. Mod. Phys. E* **22**, 1330017 (2013), 1304.2813.
- [24] B. Schmookler et al. (CLAS Collaboration), *Nature* **566**, 354 (2019).
- [25] G. A. Miller, *Phys. Rev. Lett.* **123**, 232003 (2019), 1907.00110.
- [26] E. P. Segarra, A. Schmidt, D. W. Higinbotham, E. Piasetzky, M. Strikman, L. B. Weinstein, and O. Hen, *Phys. Rev. Lett.* (2020), 1908.02223.
- [27] M. Kortelainen and J. Suhonen, *Phys. Rev. C* **75**, 051303 (2007), 0705.0469.
- [28] M. Kortelainen and J. Suhonen, *Phys. Rev. C* **76**, 024315 (2007), 0708.0115.
- [29] J. Menendez, A. Poves, E. Caurier, and F. Nowacki, *Nucl. Phys. A* **818**, 139 (2009), 0801.3760.
- [30] F. Simkovic, A. Faessler, H. Muther, V. Rodin, and M. Staaf, *Phys. Rev. C* **79**, 055501 (2009), 0902.0331.
- [31] O. Benhar, R. Biondi, and E. Speranza, *Phys. Rev. C* **90**, 065504 (2014), 1401.2030.
- [32] R. Cruz-Torres, A. Schmidt, G. A. Miller, L. B. Weinstein, N. Barnea, R. Weiss, E. Piasetzky, and O. Hen, *Phys. Lett. B* **785**, 304 (2018), 1710.07966.
- [33] X. B. Wang, A. C. Hayes, J. Carlson, G. X. Dong, E. Mereghetti, S. Pastore, and R. B. Wiringa, *arXiv* (2019), 1906.06662.
- [34] C. Ciofi degli Atti and S. Simula, *Phys. Rev. C* **53**, 1689 (1996).
- [35] R. Weiss, B. Bazak, and N. Barnea, *Phys. Rev. C* **92**, 054311 (2015), 1503.07047.
- [36] M. Alvioli, C. Ciofi degli Atti, and H. Morita, *Phys. Rev. C* **94**, 044309 (2016).
- [37] R. Weiss, R. Cruz-Torres, N. Barnea, E. Piasetzky, and O. Hen, *Phys. Lett. B* **780**, 211 (2018).
- [38] R. Weiss, I. Korover, E. Piasetzky, O. Hen, and N. Barnea, *Phys. Lett. B* **791**, 242 (2019), 1806.10217.
- [39] O. Hen, L. B. Weinstein, E. Piasetzky, G. A. Miller, M. M. Sargsian, and Y. Sagi, *Phys. Rev. C* **92**, 045205 (2015).
- [40] C. Ciofi degli Atti and H. Morita, *Phys. Rev. C* **96**, 064317 (2017), 1708.05168.
- [41] M. Alvioli, C. Ciofi Degli Atti, L. P. Kaptari, C. B. Mezzetti, and H. Morita, *Int. J. Mod. Phys. E* **22**, 1330021 (2013), 1306.6235.
- [42] R. Cruz-Torres, D. Lonardonì, R. Weiss, N. Barnea, D. W. Higinbotham, E. Piasetzky, A. Schmidt, L. B. Weinstein, R. B. Wiringa, and O. Hen, *arXiv* (2019), 1907.03658.
- [43] G. A. Miller, A. Beck, S. May-Tal Beck, L. B. Weinstein, E. Piasetzky, and O. Hen, *Phys. Lett. B* **793**, 360 (2019), 1805.12099.
- [44] B.-A. Li, B.-J. Cai, L.-W. Chen, and J. Xu, *Prog. Part. Nucl. Phys.* **99**, 29 (2018), 1801.01213.
- [45] O. Hen, B.-A. Li, W.-J. Guo, L. B. Weinstein, and E. Piasetzky, *Phys. Rev. C* **91**, 025803 (2015).
- [46] I. Vidaña, A. Polls, and C. m. c. Providência, *Phys. Rev. C* **84**, 062801 (2011).
- [47] L. Frankfurt, M. Sargsian, and M. Strikman, *International Journal of Modern Physics A* **23**, 2991 (2008).
- [48] M. M. Sargsian, T. V. Abrahamyan, M. I. Strikman, and

- L. L. Frankfurt, Phys. Rev. C **71**, 044615 (2005).
- [49] J. R. Pybus, I. Korover, R. Weiss, A. Schmidt, N. Barnea, D. W. Higinbotham, E. Piasezky, M. Strikman, L. B. Weinstein, and O. Hen (2020), 2003.02318.
- [50] L. Weinstein and S. Kuhn, DOE Grant DE-SC0006801 (2016).
- [51] H. Hakobyan et al., Nucl. Instrum. Meth. **A592**, 218 (2008).
- [52] B. A. Mecking et al., Nucl. Instrum. Meth. **A503**, 513 (2003).
- [53] M. D. Mestayer et al., Nucl. Instrum. Meth. **A449**, 81 (2000).
- [54] E. S. Smith et al., Nucl. Instrum. Meth. **A432**, 265 (1999).
- [55] G. Adams et al., Nucl. Instrum. Meth. **A465**, 414 (2001).
- [56] M. Amarian et al., Nucl. Instrum. Meth. **A460**, 239 (2001).
- [57] R. B. Wiringa, V. G. J. Stoks, and R. Schiavilla, Phys. Rev. C **51**, 38 (1995).
- [58] A. Gezerlis, I. Tews, E. Epelbaum, S. Gandolfi, K. Hebeler, A. Nogga, and A. Schwenk, Phys. Rev. Lett. **111**, 032501 (2013), 1303.6243.
- [59] T. De Forest, Nucl. Phys. **A392**, 232 (1983).
- [60] C. Colle, W. Cosyn, and J. Ryckebusch, Phys. Rev. **C93**, 034608 (2016).
- [61] O. Hen et al. (CLAS Collaboration), Phys. Lett. **B722**, 63 (2013).
- [62] C. Colle et al., Phys. Rev. C **92**, 024604 (2015).
- [63] M. Duer et al. (CLAS Collaboration), Phys. Lett. **B797**, 134792 (2019), 1811.01823.
- [64] O. Hen et al., Jefferson Lab Approved Experiment E12-17-006A (????).
- [65] S. Gandolfi, J. Carlson, and S. Reddy, Phys. Rev. **C85**, 032801 (2012), 1101.1921.